

Structural, Petrographical and Geochemical Characterization of Tin-Tantalum Bearing Pegmatites from Chessu Area, North Central, Nigeria

*A.S. Usman¹, A.S. Boaz², S. Iyakwari¹, I.A Adegoke², A. Yohanna¹, I.Y. Anzaku¹, A.O. Lucy¹, A.M. Kaura¹, M.S. Idris¹ L.P. Kenda³, I.I. Rufai⁴ and A.I. Okkoh⁵

¹Department of Geology, Federal University of Lafia, Nasarawa State, Nigeria

²Department of Geology and Mining, Nasarawa State University, Keffi, Nigeria

³Department Physics, Taraba State University, Jalingo, Nigeria

⁴Department of Building Technology, Federal Polytechnic Ngodo-Isuochi, Abia State, Nigeria

⁵Department of Geological Technology, Isa Mustapha Agwai Polytechnic, Lafia. Nasarawa State, Nigeria

doi: <https://doi.org/10.37745/bjesr.2013/vol13n26690>

Published May 10, 2025

Citation: Usman A.S., Boaz A.S., Iyakwari S., Adegoke I.A., Yohanna A., Anzaku I.Y., Lucy A.O., Kaura A.M., Idris M.S., Kenda L.P., Rufai I.I. and Okkoh A.I. (2025) Structural, Petrographical and Geochemical Characterization of Tin-Tantalum Bearing Pegmatites from Chessu Area, North Central, Nigeria, *British Journal of Earth Sciences Research*, 13 (2),66-90

Abstract: *Granodiorite, medium grain granite gneiss, medium grain banded gneiss with pegmatite intrusion, comprise the Basement Complex rocks of Chessu. The primary geological structures that emerge from the Pan Africa ductile and brittle deformation stages are fold, strike slip fault, dextral shear plane and fractures in Chessu and environs. Tin and tantalum containing pegmatites are found in the main E-W and NE-SW fault. Field observation demonstrate NE-SW, NNE-SSW and N-S structural trend with dipping values ranging between 19°-52° in accordance with data collected, displayed on rose plots and equally supported by lineaments. In terms of petrography, medium grained banded gneiss, medium grain granite gneiss and granodiorite all contain quartz, plagioclase, biotite and muscovite. Pegmatite contains muscovite, biotite, quartz and orthoclase among other opaque minerals. The protoliths of the gneisses, which may be from granite are revealed by the geochemical data used on Middlemost plots ($Na_2O + K_2O$ vs SiO_2), which suggest that the rocks are members of the granitoid family. The Harker's variation Plots of SiO_2 vs Na_2O , K_2O , CaO , MgO , TiO_2 , P_2O_5 , reveals intense alteration and contamination during fractionation of the rock, as displayed by the scattered/non-linear trends. The primitive mantle (spider plot) indicates the depletion of some compatible less mobile elements (Ti, Y, Zr and Sr) and enrichment of incompatible elements (Th, Rb, Nb, Ta, Sr and Pb), which reveal the mineralization potential in these incompatible elements. The enriched elements Th, Nb, Ta and Pb are used as the pathfinder elements for Tin and Tantalum mineralization in Chessu area. The deformation processes and structures created in the latter phase of Pan Africa Orogenic event resulted in the pegmatite emplacement, this could infer a connection between the mineralizing fluid and the rocks.*

Keyword: Chessu, enrichment, geochemical, petrography, mineralization

INTRODUCTION

Nigeria has a long history of exploration and has abundant metallic and non-metallic resources. Nigeria is one of the African countries with substantial mineral resource potential (Mohamed, 2022). A nation's capacity to locate, utilize, and manage its mineral resources has a direct impact on its living standards, such as the case of Australia and Canada. Rocks and minerals that surround us are utilized in our daily lives and to create new technology. Rocks and minerals are used in construction, cosmetics, automobiles, highways, and appliances. Also, humans require daily mineral consumption to strengthen the body and sustain a healthy lifestyle.

The Nigerian mining and exploration industry need creative methods to address the challenges of declining mineral resources and growing discovery costs since the lucrative mining opportunities in easily accessible metalliferous and non-metalliferous environments are rapidly dwindling, exploration experts are shifting their attention to the incredibly under-explored, often challenging, and inaccessible places. Mineral exploration is a multidisciplinary team effort that involves various experts including geophysicists, geochemists, geologists, petrologists, mining engineers, metallurgists, geostatisticians, environmental scientists/ecologists, GIS analyst, and other related disciplines. Discovery of mineral deposits has been made possible in many parts of the world using geochemical techniques (Balaram & Sawant, 2022), integrated with several other geoscientific exploration techniques.

In pursuit of lucrative ore deposits, the structural, geological, mineralogical, and geochemical characteristics of rocks and mineralized zones are frequently exploited. According to Lowrie and Fichtner (2020), the reason for this is because mineralized zones frequently display unusual geo-spectral, geophysical, mineralogical, geological, structural, and geochemical characteristics that enable their characterization. By combining structural, petrographical, and geochemical techniques, numerous mineral deposits have been found (Paulen et al., 2009; Chakraborty et al., 2020; Azmi et al., 2021; Balaram & Sawant, 2022). However, it is important to keep in mind that determining the exact geological size and extents of an ore body using single method is insufficient and often challenging, making the identification of mineralized zones often beset with uncertainty (Ombiro & Akisa, 2016). Depending on the properties of the host rock and mineralization, incorporating a variety of techniques is the best way to reduce this uncertainty (i.e., to prove beyond a reasonable doubt) (Auken et al., 2006; Vallee et al., 2011).

There have been numerous reports of base metal occurrences, including tin, tantalum, in various parts of Nigeria (Mohamed, 2022). Tin and tantalum are among the most common minerals that artisanal miners primarily extract from primary place of origin and secondary placer deposits. Nigeria currently mines primary tantalum and tin; some projects have advanced beyond exploration stage and are starting the pre-mining phase; they may become the next mines in a few years. Despite her continued under-exploitation of its metallic and industrial mineral reserves, including tin and tantalum, significant exploration efforts have been conducted by the Nigerian Geological Survey Agency (NGSA) and other private exploration companies.

Thus far, mineral exploration attempts in the study area have failed to find surface and subsurface mineralization perhaps due to limited knowledge about the structural controls, origin, the

Publication of the European Centre for Research Training and Development -UK mineralized lithology and the vectors towards economic Tin-Tantalum mineralization within the study area. Artisanal tin and tantalum mining in the Chessu area is being driven by a more significant issue such as market liberalization, economic hardship and structural adjustment which have "induced significant unemployment rate thereby forcing many people into illegal mining to supplement their incomes. This study was conducted in order to map out the potential mineralized lithology- pegmatites, their host rocks, structural control, mineralogy, and elemental composition of the mapped lithologies in the area.

Study Area Location, Geological setting, and Geomorphology

The area is situated in Wamba local Government, Nasarawa State, Northcentral Nigeria. It lies between latitudes 9°03'20" N to 9°06'40" N and longitudes 8°35'00" E to 8°40'00" E, with an approximate land mass of 50km² (Figure 1). Based on the geology, the area is underlain by the Pan-African Basement rocks, which are a component of the Upper Proterozoic-Lower Phanerozoic mobile belt that runs between the Congo Cratons in the southeast and the West African Craton in the west (Dada, 2008). The rocks of the Basement Complex are divided into two groups: those belonging to the Migmatite Gneisses Complex (medium grain banded gneiss and medium grain granite gneiss) and those belonging to the Older Granite suits (granodiorite with pegmatite intrusion) and patches of micro veins of basaltic rocks (Figure 2). The area is an extension of Sha-Kaleri Complex. Based on field observations, it is possible that the granodiorites in the area might have intruded the country rocks, causing gneissification of the country's rocks. The pegmatite veins intruding the gneisses (Medium grain banded gneiss and Medium grain granite gneiss) displayed NE-SW, NE-SW NNW-SSW trends, while the pegmatite around the granodiorite forms dooms to flat lying outcrops. Majority of streams are structurally controlled, based on structural and aeromagnetic data of North Central Nigeria (Anudu et al., 2010), this suggest the likelihood for the mineralization in the study area to be also structurally controlled.

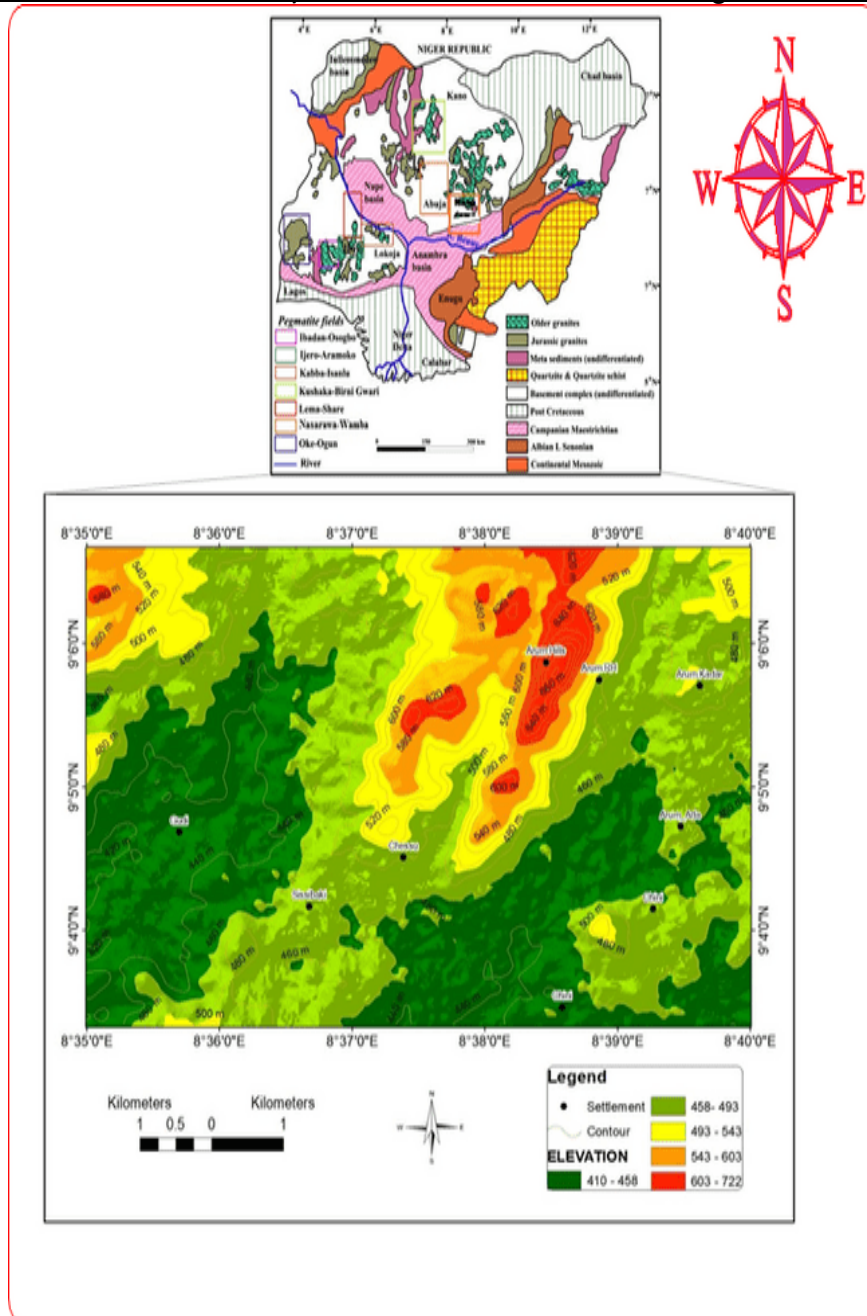


Figure 1: A satellite imagery map of the Arum part of Kura sheet 189, indicating the topography of the study area. The study area is indicated in a purple color in the geological map of Nigeria modified after Okunlola 2009.

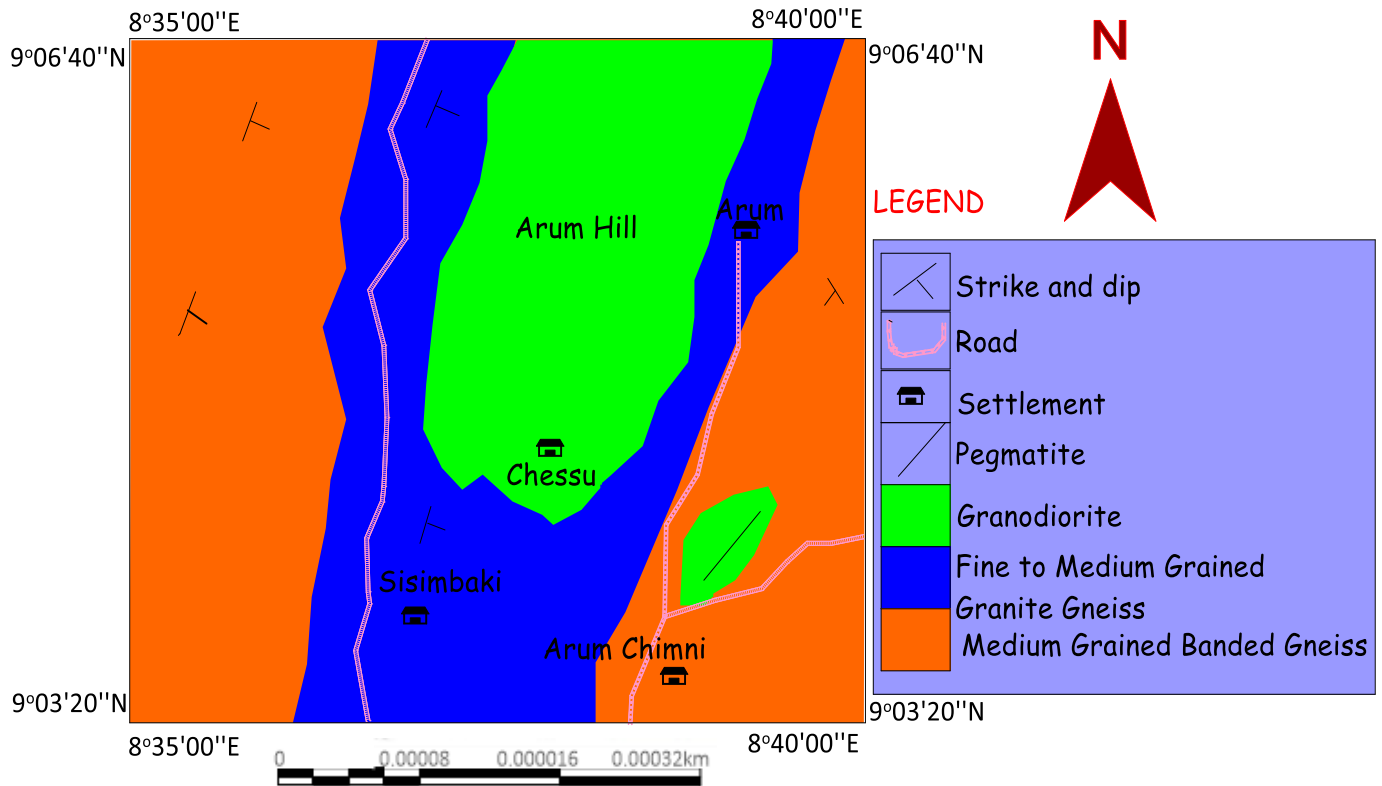


Figure 2: Geological map of the study area.

MATERIALS AND METHODS

The following materials were used in this study: a geological pick/sledge hammer, a compass-clinometer, a pen, a field notebook, a measuring tape, sample bags, permanent markers, masking tape, GPS, and a base map that indicates the locations of all natural and man-made features.

Geology, Structural Measurement and Lineaments Characterization from Aeromagnetic Data

To generate the area's lineament map and Rose diagram, lineaments were collected from Kura Sheet 189's aeromagnetic data during the desk study. The objective is to identify pegmatites' position and their tendencies. During the fieldwork, the discovered lineaments served as control locations for the sampling of pegmatites. Representative pegmatite samples were collected at each point along veins indicated on the aeromagnetic map that might contain mineralization. Using a 100 m by 100 m square grid, samples were collected along profiles perpendicular to the trending direction of the structures. Plotting Rose diagrams required taking notice of the structures' attitudes.

Petrography and Geochemistry

About sixteen (16) fresh (unweathered) samples were collected along veins. The megascopic samples were used for textural features, color, mineralogy and mineral orientation. The laboratory work involved sample preparation for petrographic and geochemical analysis. Software (Surfer) application was equally adopted for data plotting and digitization. The petrographic investigation was conducted at the Petrographic Laboratory of the Department of Geology & Mining, Nasarawa

Publication of the European Centre for Research Training and Development -UK State University, Keffi, Nigeria, using a petrological microscope. The XRF analysis for elemental composition was carried at the Center for Solid Mineral Research and Development (CSMRD) at Kaduna, Kaduna State, Nigeria.

RESULTS AND DISCUSSIONS

Structural Characterization of the Area

Among the structures studied are veins, foliation, joints, xenolith, folds, faults, and exfoliation. A compass clinometer was used to measure the orientation of these structures, which were thoroughly examined. The granodiorite on Arum Hill showed signs of exfoliation, which could be the result of weathering-related physical and chemical processes or other denudational activity. In the banded gneisses, fold was primarily seen. It can be concluded that the foldings were caused by the pressure and heat from the nearby ring complexes (Shakaleri and Mada) or the heat released during the granodiorite intrusion, or a combination of both. Additionally, the folding of the gneisses may have been caused by Pan African orogenic activities. Ptygmatic folding, which only appears in the medium-grain banded gneiss exposed along a river channel south of Chini town, is another noteworthy structural feature in the studied area. In the study area, quartz and quartzofeldspathic veins were found in the rock. The majority of these veins run parallel to the overall NNE-SSW (Figure 3) orientation and come in a variety of sizes. Based on the kind of crystallized minerals, the veins in Arum can be divided into two main categories: recrystallized rock that is rich in feldspar and quartz, which gives rise to quartzofeldspathic veins, and the in-filled cavity caused by the precipitation of leftover fluids. Additionally, the medium grain banded gneiss exhibited foliation. Both the medium-grained granite gneisses and the granodiorite gneisses showed joint. In accordance with the trend derived from ground measurements, the lineament map generated from the aeromagnetic data shows that the primary structural trends are NE-SW and NNE-SSW, with minor components in the N-S trend (Figures 4 and 5). Similar patterns are also seen in field measurements, with 40° to 45° dips predominating (Figure 5b). The findings also reveal that the structures range from 2m to more than 100 m, with the former being limited as major faults. These patterns are similar to those found in the north-eastern portion of the Nigerian Basement Complex (e.g., Bassey, 2006) and field measurements. The lineaments in the area point to a complicated tectonic past, with a high degree of fracture. The lineaments were primarily found in the central, southern, north-east, and south-east regions Fig 4 . High lineament density zones are essential for the location of mineral deposits (Andarawus et al., 2023a, Ananaba & Ajakaiye, 1987).

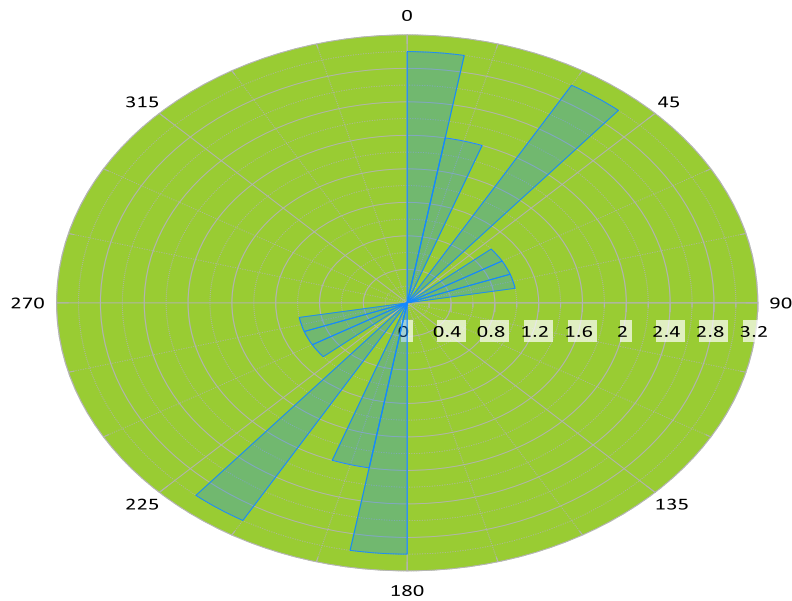


Figure 3: Rose diagram showing orientations of veins in the study area.

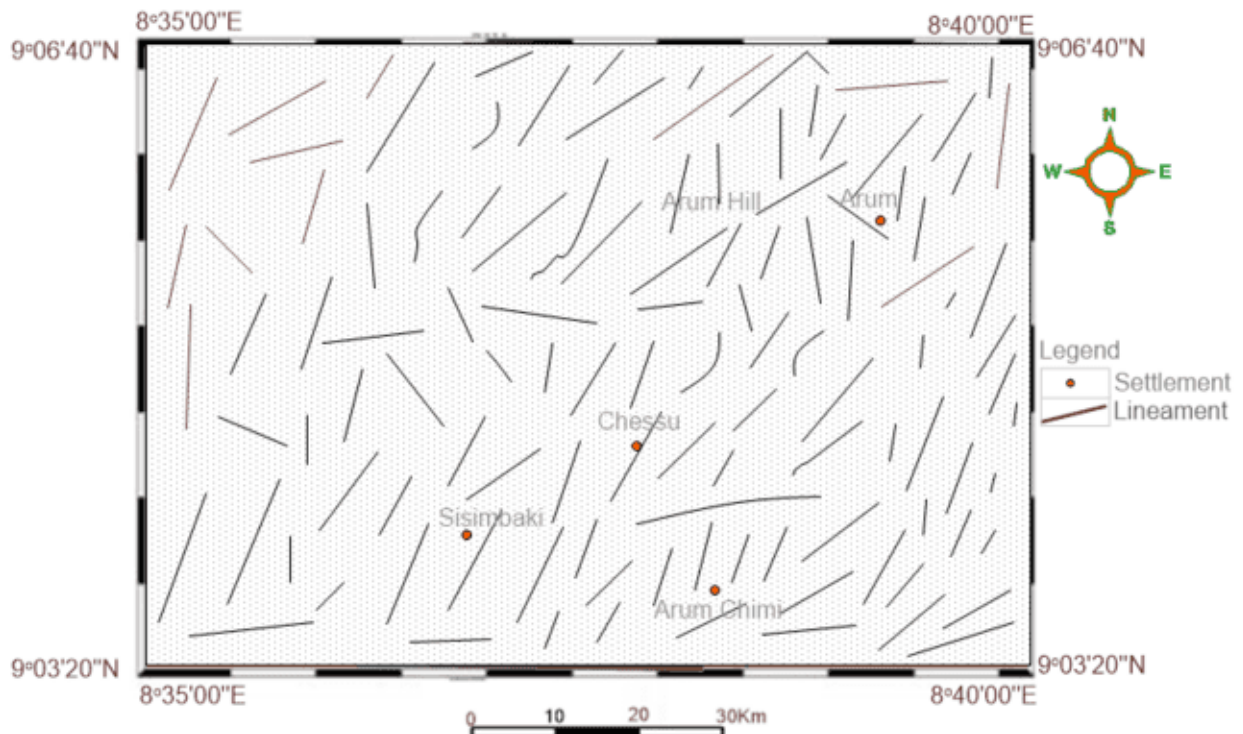


Figure 4: Lineament map of the area showing orientations of veins extracted from aeromagnetic.

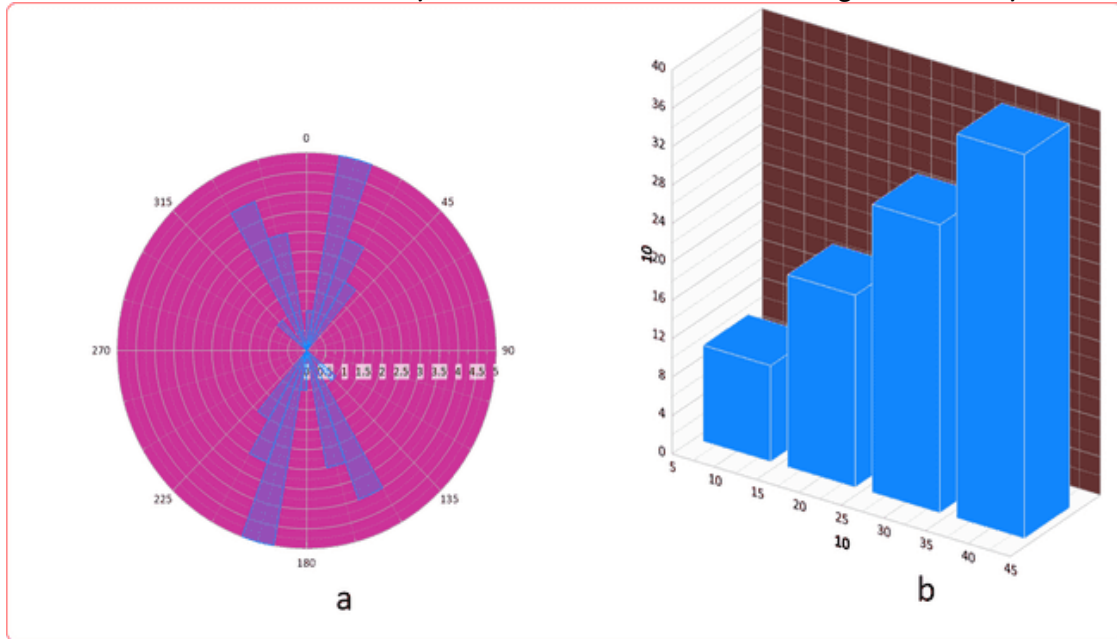


Figure 5: (a) Rose diagram showing orientation of pegmatites in the area (b) Histogram of dips of pegmatites in the area.

Lithological study and field relationship

Granodiorite (G), medium-grained banded gneiss (MGBGn), and fine to medium-grained granite gneiss (FMGGn) are the three main rock types found in the area. Pegmatite and vein-let basalt have also been found to intrude some of the host rocks in the area. Field observation indicates that granodiorite intruded the granite, changing its textural and mineralogical properties and causing the emplacement of fine to medium grained granite gneiss. Granodiorite formed a hilly and mountainous altitude Fig 7a The medium grained banded gneiss has more metamorphic features than the medium grain granite gneiss, according to field studies. This phenomenon may clearly demonstrate that the medium grained banded gneisses' textural and structural adjustment may have been influenced by the nearby Ring Complex (Sha-kaleri and Mada) or may have been exposed to relatively more intense metamorphic processes.

Pegmatite

Pegmatite is an interesting aspect of the geology of the area. Two forms of pegmatite have been mapped in the study area based on field relations and manner of occurrence. The first type of pegmatite is type-1, which is large, zoned, oval-shaped, and has a ridge-trending NE-SW orientation. It is found in the northern part of Arum Chinni, which is part of the Chinni hill, which has a long history of mining activity. Type-II pegmatite, the second category, is characterized by tiny veins that primarily strike in NE-SW directions. In their host rocks, these pegmatites appear as veins (Figure 6a). In line with the overall structural tendency in the region, the veins are roughly 15 to 25 cm thick and primarily trend NE-SW. The two main minerals found in the hand specimen are quartz and plagioclase, with muscovite appearing as a minor component.

Pegmatite thin sections and petrographic analyses reveal the presence of quartz, biotite, plagioclase, and muscovite (Figure 6b). Quartz is a mineral that appears as grey in cross-polarized light and as colorless to hazy in normal polarized light. Anhedral shapes exhibit pleochroism, low relief, and no cleavage or change. Coarse, elongated plates of muscovite are light brown in

Publication of the European Centre for Research Training and Development -UK
 ordinary polarized light and dark brown in crossed polarized light. It can be found in the intergranular gaps of quartz crystals that lock together. Subhedral grains of biotite are found between crystals of other minerals; they are brownish in plain polarized light and nearly black in cross polarized light. They are pleochroic, lineated (prism and platy), have one path of cleavage, and modest relief. With a low relief, prismatic shape, oblique extinction lamellar twinning pattern, and no discernible cleavage, plagioclase appears colorless in plain polarized light but hazy and grey in crossed polarized light, (Table 1: Modal Estimation of rocks and their compositions in the study area).



Figure 6: (a) Pegmatite exposure in Arum Chinni (b) Photomicrograph of pegmatite. B= Biotite, MV= Muscovite, P= Plagioclase Feldspar, Q= Quartz.

Table 1: Modal Estimation of rocks and their compositions in the study area.

Rock Types/Minerals	Pegmatite composition (%)	Granodiorite composition (%)	Fine to medium grained banded gneiss composition (%)	Medium grained granite gneiss composition (%)
Quartz	26.9	27	22.6	27.3
Plagioclase	27.3	31.2	36.3	36.1
Biotite	24.1	13	19.2	21.1
Muscovite	12.3	11	19.9	-
Albite	+ 9.1	-	-	-
Orthoclase	-	-	-	-
Microcline	+ -	16.1	-	13.5
orthoclase	-	-	-	-
Accessory minerals	-	1.2	-	1.9
Orthoclase (K-Feldspar)	-	-	2.7	-
Total	99.8	99.8	99.8	99.8

Granodiorite

About 25% of the area is made up of 800-meter-high granodiorite, with large boulders on the hill's summit and a coarse-grained, leucocratic texture. It is further distinguished by the rock's equal exfoliation (Figure 7a). Granodiorite thin sections and petrographic analysis reveal the presence of plagioclase feldspar, quartz, biotite, muscovite, and other opaque minerals (Figure 7b). Due to alteration, alkali feldspar (orthoclase) looks filthy and has a subhedral to euhedral shape. Cross-polarized light gave the plagioclase a dark to gray appearance, low relief, and a colorless appearance. Many exhibit the texture of micro-perthite. Biotite exhibits significant pleochroic characteristics in pale streak and dark reddish brown with speckled extinction under plane polarized light (PPL), with no preferential alignment. No twinning was seen, and the quartz had a very low relief, euhedral shape and seemed colorless and poorly pleochroic. Some sections exhibit cleavage of biotite, phenocrysts of microcline set in groundmass of quartz, plagioclase, and biotite. Biotite displayed a brown to dark color, little alteration, and no twinning. It goes extinct when the stage is rotated. According to Nanfa et al., (2023), the microcline showed twinning and a gray interference color without any extinction angle. Iron oxide and zircon are the accessory minerals, (Table 1: Modal Estimation of rocks and their compositions in the study area).



Figure 7: (a) Granodiorite exposure showing exfoliation in Arum chinni (b) Photomicrograph of Granodiorite. B= Biotite, M= Microcline, O= Opaque Minerals, P= Plagioclase Feldspar, Q= Quartz.

Fine to Medium Grained Granite Gneiss

About 30% percent of the study area is covered by fine to medium grained granite gneiss. Field observation shows that, granodiorite intruded the protolith of the fine- to medium-grained granite gneiss (Figure 8a) and resulted to its gneissification. It can be deduced that the Sha-Kaleri Ring Complexes and the granodiorite intrusions contribute to the textural, structural, and mineralogical readjustment of the gneisses around Chessu. Quartz, Biotite, Plagioclase, and Muscovite are the minerals found in fine to medium granite gneiss, according to petrographic analysis (Figure 8b). In comparison to other minerals, quartz had a subhedral crystal structure and appeared colorless and non-pleochroic under plane polarization. The crystal structure of Plagioclase was subhedral, low relief, colorless, and non-pleochroic (Mu'awiya et al., 2022). Muscovite exhibits cleavage with a subhedral structure, but biotite seems flappy, brown to dark, and exhibits modest relief and pleochroism. Under cross-polarized light, muscovite displayed an interference color that was grey

Publication of the European Centre for Research Training and Development -UK without extinction. Biotite becomes extinct as its turns brown without changing or twinning. Quartz showed interference color without twinning or any other indication of change. Interference color is displayed by plagioclase without any distinct twinning, (table 1 shows the percentage modal composition of fine to medium grained granite gneiss).



Figure 8: (a) Exposure of fine to medium grained granite gneiss (b) Photomicrograph showing fine to medium grained granite gneiss. B= Biotite, M= Muscovite, P= Plagioclase Feldspar, Q= Quartz

Medium Grained banded gneiss

About forty-three (43%) of the study area is made up of medium-grain banded gneiss, which had an average elevation of 480 meters and a medium-grained texture (Figure 9). It is thought to have formed as a result of pressure from the weight of the rocks above it or as a result of the Sha-kaleri and Mada Ring Complexes' orogenic activities. The heat from the intrusion of a volcanic body that is not exposed to the surface, or rather, magma intrusion, and creating separate felsic and mafic bands that range in size from a few millimeters to tens of centimeters. As a result, micro quartzo-feldspathic veins and micro basaltic dykes appeared within the medium grained banded gneiss.

Petrographic and thin section analyses of medium grain banded gneiss reveal the main minerals as quartz, orthoclase, and plagioclase feldspar (Figure 9b). Very coarse-grained crystals of quartz are found (Odinaka et al., 2023). Feldspar occurs as plagioclase. Biotite is part of the major constituent while muscovite occurs as colorless flaky aggregate from the microphotograph. Quartz is colorless, subhedral, and low relief without cleavage or twinning. Plagioclase crystals are subhedral, low relief, and hazy pattern. With a pale surface or patches, the orthoclase which occur as a minor mineral exhibits Carlsbad twinning, most likely as a result of weathering changes. The orthoclase feldspar is found at the interface between the plagioclase and quartz and or muscovite. Subhedral biotite, which exhibits pleochroism from brown to yellow, is found sporadically among crystals of feldspar and quartz, (Table 1: Modal Estimation of rocks and their compositions in the study area).

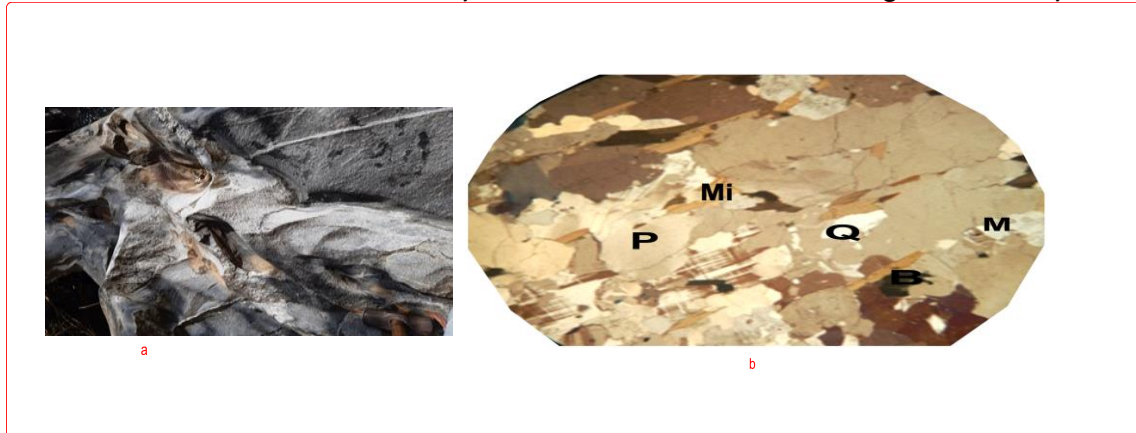


Figure 9. (a) Medium grain banded gneiss with spheroidal weathering along river Gudi of the study area (b) Photograph showing medium grain banded gneiss. M= Muscovite, Mi= Microcline, P= Plagioclase Feldspar, Q= Quartz.

Geological structures observed in the study area

Exfoliation, veins, folds, foliation, and joints are among the structures mapped in the study area. They mostly strike in NE-SW lines, while a few small cracks also trend in E-W directions. The fractures affected the granodiorite but are more common in the medium grained banded gneiss. Another notable structural feature in the study area is ptygmatic folding, which occurs exclusively in the banded gneiss exposure along a river channel, south of Chini village.

Fold

The fold around the rocks in the study area varies in size, appearing as isolated folds or periodic sets, and appeared as a stack of initially flat surfaces that were likely bent or curled during permanent deformation (Figure 10).



Figure 10: Ptygmatic folding observed on the gneiss.

Veins

The veins in the study area have a noticeable sheet-like body of its recrystallized minerals. The minerals that comprise the rocks may be carried by an aqueous solution and deposited by precipitation to form them. The dominant veins, as observed from the field have characteristic features of ore deposits that are scattered within specific borders of different alternating rock

Publication of the European Centre for Research Training and Development -UK minerals and or gangue. The rock in the study area contains both quartz and quartzo-feldspathic veins, the majority of which run parallel to the main NW-SE orientation and varied in size throughout the study area (Figure 11).



Figure 11:
Quartzo-

feldspathic vein observed at southern Arum Chinni river.

Exfoliation

The weathering of rocks by the separation of successive thin shells from the large body of the granodiorite may be the cause of the exfoliation seen in the field. As observed from field study, the variations in individual sheet thickness ranging from millimeters to meters, shows a typical exfoliation structure (e.g., Figure 7a) which have occurred parallel to the rock's outer surface, probably due to combination of chemical breakdown of minerals or as a result of mechanical weathering, or a combination of both.

Xenolith

According to field study, the xenolith in the study region may be trapped or subsume as observed near or within a feldspathoid body, which is a rock that is trapped in another kind of rock. Additionally, it could be a piece of rock that develops into a larger boulder as it grows and solidifies. It is consistently referred to as an inclusion in igneous rock that is entrained during the eruption, emplacement, and ascent of magma. figure 12 below shows an inclusion of gneiss in a quartzo feldspathic rock along river chinni of the study area.



Figure 12. Xenolith (a gneiss inclusion in quartzo-feldspathic rock expose along a river southern Chini village.

Joint

A joint is a brittle-fracture surface in rocks along which little or no displacement has occurred. The joints observed in the field were dominantly found around the granodiorite as pronounced fractures or cracks (Figure 13). Lateral movement between the joints seen on granodiorite is minimal or non-existent.



Figure 13a(i and ii): Photograph showing a joint on the granite around Arum Hill of the study area.

Geochemistry of rocks observed in the study area

A total of sixteen (16) samples, four for each rock type, were subjected to major, trace, and base metal analysis (Table 2). These consists of pegmatite, medium-grained banded gneiss, fine- to medium-grained granite gneiss, and representative examples of granodiorite. An X-ray fluorescence spectrophotometer was used for geochemical analysis of the representative rock samples. Rock software and GeoChemical Data (GCDkit) was used for data plotting and visualisation.

Major oxides geochemistry of the study area

A tremendous anomaly for mineralization is shown by the geochemical data analysis of the mineralized rock samples. The results indicate that the shear zone altered metamorphic rocks contain certain anomalies in the content of quartz, iron, and titanium (Table 2). RK1 = Medium grained banded gneiss ,RK2 = Pegmatite, RK3 = Pegmatite, RK4 = Medium grained banded gneiss, RK5 =Medium grained banded gneiss, RK6 = Medium grained banded gneiss , RK7 = Fine to medium grained granite gneiss, RK8 = Fine to medium grained banded gneiss , RK9 =Fine to medium grained granite gneiss ,RK10 = Fine to medium grained granite gneiss , RK11 = Fine to Medium grained granite gneiss , RK12 = Granodiorite , RK13 = Granodiorite, RK14 = Granodiorite , RK15 = Pegmatite, RK16 = Medium grained banded gneiss Silica (SiO₂) content ranges from 64.82 to 77.14%, aluminum oxide (Al₂O₃) ranges from 13.26 to 15.91%, ferric oxide (Fe₂O₃) ranges from 0.74 to 6.56%, sodium oxide (Na₂O) ranges from 0.49 to 5.35%, potassium oxide (K₂O) ranges from 0.77 to 5.61%, calcium oxide (CaO) ranges from 0.12 to 5.49%, magnesium oxide (MgO) ranges from 0.16 to 3.62%, titanium dioxide (TiO₂) ranges from 0.01 to 2.01%, manganese oxide (MnO) ranges from 0.03 to 0.32%, phosphorous pentoxide (P₂O₅) has concentrations of 0.01 to 0.80%, and loss on ignition (LOI) ranges from 0.1 to 1.85% (Table 2).

Publication of the European Centre for Research Training and Development -UK

The average major elements of all the samples show that SiO₂ (72.53%) is the most common element, with considerable contributions from Al₂O₃ (14.47%), and then minor contributions from Fe₂O₃ (2.73%), Na₂O (2.28%), K₂O (3.32%), CaO (2.48%), and MgO (1.17%). Other oxides, including TiO₂, MnO, P₂O₅ are very low in the rocks- < 1% (Table 2).

The findings showed that the two most prevalent main oxides in the rocks are SiO₂ and Al₂O₃. Al₂O₃ indicates the high presence of aluminosilicate-bearing minerals like feldspar, micas, and feldspathoids, while SiO₂ indicates that the rocks are dominantly siliceous. Generally, the result of the geochemical analysis shows that all samples have significant concentrations of SiO₂ and Al₂O₃ which agrees with the composition of most silicic-intermediate igneous rocks and metamorphic rocks such as gneiss and migmatite. Most of the rocks are intermediate to felsic.

All the samples show quite consistent distribution patterns (Table 2). The samples' fingerprints are largely provided by the compositionally high concentration of SiO₂ and Al₂O₃. A shared protolith or petrogenetic past is hereby suggested based on the results of the geochemical analysis of the representative rock samples.

Table 2: Major oxide geochemical analysis of rocks in the area (W%).

S/N	Sample ID	Rock Type	SiO ₂	Al ₂ O ₃	Fe ₂ O ₃	Na ₂ O	K ₂ O	CaO	MgO	TiO ₂	MnO	P ₂ O ₅	LOI	Total
1	RK1	MBBG	68.5	14.3	4.98	0.58	0.98	4.51	3.47	2.01	0.32	0.04	0.33	99.98
2	RK2	Pg	70.57	13.48	1.08	2.38	4.98	5.49	0.64	0.94	0.04	0.06	0.49	99.95
3	RK3	Pg	75.93	13.26	1.21	2.11	5.01	1.02	0.92	0.31	0.04	0.01	0.18	100.00
4	RK4	MBBG	74.13	14.38	3.89	2.41	1.24	2.41	0.41	0.7	0.13	0.02	0.28	100.42
5	RK5	MBBG	77.14	14.65	0.74	2.14	4.03	0.15	0.56	0.02	0.14	0.01	0.42	100.04
6	RK6	MBBG	68.34	15.02	4.66	0.49	0.77	4.72	3.62	1.86	0.12	0.03	0.37	100.00
7	RK10	FMGGG	76.82	14.47	0.79	2.38	4.3	0.14	0.55	0.03	0.16	0.20	0.35	99.80
8	RK12	FMGGG	76.09	14.13	0.93	2.09	5.07	0.44	0.43	0.01	0.11	0.06	0.74	99.940
9	RK13	FMGGG	64.82	15.69	6.56	2.62	1.81	5.04	1.65	1.85	0.31	0.80	1.23	99.20
10	RK16	FMGGG	73.02	15.06	3.85	2.38	1.24	2.35	0.41	0.65	0.16	0.03	1.85	99.15
11	RK17	FMGGG	72.92	14.26	0.85	2.2	5.61	2.09	2.49	0.04	0.14	0.10	0.82	99.90
12	RK18	Gr	69.21	15.91	5.62	5.35	2.55	2.37	0.54	0.78	0.07	0.02	1.13	101.00
13	RK22	Gr	66.24	14.81	5.46	2.55	1.79	5.04	1.61	1.85	0.30	0.35	1.35	100.65
14	RK28	Gr	75.76	13.74	1.03	2.17	4.65	1.85	0.16	0.46	0.03	0.05	1.10	101.00
15	RK30	Pg	74.09	14.07	1.04	2.41	5.06	1.91	0.73	0.5	0.06	0.03	0.10	100.00
16	RK34	MGBG	76.95	14.35	1.01	2.21	3.98	0.12	0.58	0.03	0.17	0.01	0.59	100.00
	Minimum		64.82	13.26	0.74	0.49	0.77	0.12	0.16	0.01	0.03	0.01	0.1	99.15
	Maximum		76.95	15.91	6.56	5.35	5.61	5.04	3.62	1.86	0.31	0.8	1.85	101
	Average		72.53	14.47	2.73	2.28	3.32	2.48	1.17	0.75	0.14	0.11	0.71	100.06

RK1 = Medium grained banded gneiss ,RK2 = Pegmatite, RK3 = Pegmatite, RK4 = Medium grained banded gneiss, RK5 =Medium grained banded gneiss, RK6 = Medium grained banded gneiss , RK10= Fine to medium grained granite gneiss, RK12 = Fine to medium grained banded gneiss , RK13 =Fine to medium grained granite gneiss ,RK16 = Fine to medium grained granite gneiss , RK17 = Fine to Medium grained granite gneiss , RK18 = Granodiorite , RK22= Granodiorite, RK28= Granodiorite , RK30= Pegmatite, RK34= Medium grained banded gneiss

Trace and Base Metals Elemental composition in the area

The content of nickel (Ni) ranges from 5.00 to 13 ppm, copper (Cu) ranges from 4 to 42 ppm, zinc (Zn) ranges from 6 to 35 ppm, barium (Ba) ranges from 127.00 to 867 ppm, niobium (Nb) ranges from 3 to 63 ppm, arsenic (As) ranges from 4 to 9 ppm, and rubidium (Rb) ranges from 101 to 370 ppm (Table 3). The ranges for strontium (Sr) and zircon (Zr) content are 236–511 ppm and 102–215 ppm, respectively (Table 3). Gold (Au) is not predetermined. The concentrations of tin (Sn) ranges from 8 to 271 ppm, cobalt (Co) from 0.5 to 25 ppm, silver (Ag) from 9 to 38 ppm, chromium (Cr) from 49 to 97 ppm, and tantalum (Ta) from 39 to 343 ppm (Table 3). Yttrium (Y) concentration ranges from 1 to 41 ppm, Vanadium concentration ranges from 7 to 94 ppm, Thorium (Th) concentration ranges from 2 to 19 ppm, Uranium (U) concentration ranges from 5 to 15 ppm, and Gallium (Ga) concentration ranges from 0.6 to 21 ppm (Table 3). The idea of geochemical background is fundamental to both geochemistry and mineral prospecting. "Normal abundance of an element in barren earth material or normal crustal abundance of material naturally" is the definition of background (Chapman et al, 2017; McClenaghan, 2005; Fortescue, 1992; Parker 1967).

An anomaly can be either positive or negative if the geochemical value differs from the background crustal abundance. Table 4 shows a comparison of the obtained average elemental values (minimum, maximum and average) against pre-established standard crustal abundance values. Tin (Sn), arsenic (As), zircon (Zr), rubidium (Rb), yttrium (Y), niobium (Nb), barium (Ba), tantalum (Ta), and silver (Ag) are the metals with levels greater than their crustal abundances, by comparing the result of the geochemical analysis with the pre-established background values for the corresponding element analysed. Since their geochemical values differ from the background crustal abundance, they have a positive anomaly that suggests possible mineralization (Andarawus et al, 2023c; Fortescue, 1992; Parker, 1967), and this warrants exploration follow up.

The spider plot in Figure 14 shows the enrichment of thorium (Th), rubidium (Rb), niobium (Nb), tantalum (Ta), and strontium (Sr), as well as the depletion of Ti and Y and the moderate depletion of Zr and Sr. These elements are anomalously concentrated in the environment. Thus, Sn, as indicated in Table 3, may also contribute to the formation of tantalite and columbite. Additionally, it was noted that pegmatite samples had a significant concentration of Sn, and that Zr, Y, and Ti exhibited negative anomalies that resembled those of pink and leucocratic granite. These anomalies could indicate that plagioclase and accessory minerals were either retained in the source during partial melting or separated during fractionation (Singh and Vallinayagam, 2012). After Middlemost 1994, the granodiorite plot falls between the metaluminous and peraluminous sectors on the molecular A/CNK against A/NK diagram (Figure 15). This rock unit's progression from peraluminous to metaluminous is a result of the continental crust contaminating magma originating from the mantle (Ustamer, 1999). According to White and Chapell (1977), peraluminous granites are mostly S-type granites, which are produced by partial melting of sedimentary protolith. In this case, the granodiorite samples that fall within the peraluminous field as shown in Figure 15 may be analogous to the peraluminous and S-type granites.

Table 3: Trace and base metals elemental composition in the area (ppm).

S/ N	Sample ID	Rb	Sr	Cr	Th	U	V	Ta	Nb	Co	Cu	Sn	Ag	Ba	Zr	Pb	Ni	Zn	Ga	Y	Ti	
																As						
1	RK1	109	236	97	8	11	7	16	12	09	13	18	12	212	113	5	-	07	06	12	4	6
2	RK2	184	437	75	19	7	19	231	58	32	19	208	11	307	110	4	2	08	09	16	27	7
3	RK3	142	392	82	13	9	26	241	66	41	34	202	09	733	106	6	1	08	11	4	11	11
4	RK4	287	413	82	4	7	18	106	21	2	13	18	21	716	103	8	13	07	08	2	14	13
5	RK5	201	311	68	14	6	51	93	16	7	41	17	35	606	111	4	1	11	35	21	25	7
6	RK6	311	374	72	2	9	23	76	7	-	39	8	18	867	118	6	18	13	06	11	32	4
7	RK10	252	502	73	19	12	94	76	48	24	21	29	36	784	127	7	3	06	34	1	24	2
8	RK12	101	279	72	9	12	16	323	4	1	35	89	15	471	104	7	1	12	15	4	3	15
9	RK13	241	511	67	7	5	14	66	12	2	13	11	22	727	126	7	6	08	10	2	21	16
10	RK16	212	407	74	4	8	11	105	23	1	42	10	21	512	102	9	7	05	09	2.4	18	13
11	RK17	198	382	94	5	9	16	117	18	08	11	40	23	127	121	6	13	05	09	0.6	2	3
12	RK18	302	402	49	5	8	13	103	12	06	4	09	21	550	108	8	3	13	11	1	1	1
13	RK22	261	426	78	13	9	61	121	3	2	24	08	16	649	197	9	11	07	07	9	7	3
14	RK28	330	491	81	4	6	24	109	63	0.5	8	93	21	365	119	8	11	08	19	7	32	2
15	RK30	293	398	59	3	9	15	343	96	29	34	271	17	486	113	9	9	10	12	12	7	1
16	RK34	370	501	77	17	15	81	73	37	3	28	64	38	812	215	9	17	07	32	14	41	4
	Min	101	236	49	2	5	7	16	3	0.5	4	8	9	127	102	4	1	5	6	0.6	1	1
	Max	370	511	97	19	15	94	343	96	25	42	271	38	867	215	9	18	13	35	21	41	16
	Ave	237.13	403.88	75.00	8.25	8.88	30.56	146.50	23.00	6.03	23.69	61.00	21.00	557.7	124.6	7.0	7.73	8.44	14.5	7.4	16.78	7.4
														5	0				6	4		

RK1 = Medium grained banded gneiss ,RK2 = Pegmatite, RK3 = Pegmatite, RK4 = Medium grained banded gneiss, RK5 =Medium grained banded gneiss, RK6 = Medium grained banded gneiss , RK10= Fine to medium grained granite gneiss, RK12 = Fine to medium grained banded gneiss , RK13 =Fine to medium grained granite gneiss ,RK16 = Fine to medium grained granite gneiss , RK17 = Fine to Medium grained granite gneiss , RK18 = Granodiorite , RK22= Granodiorite, RK28= Granodiorite , RK30= Pegmatite, RK34= Medium grained banded gneiss

Publication of the European Centre for Research Training and Development -UK

Table 4: A comparison of the obtained elemental values (minimum, maximum and average) against pre-established standard crustal abundance values.

S/N	Metal/Element	Minimum	Maximum	Average	Crustal abundance*
1	As	4	9	7	1.8
2	Ag	9	38	21	0.08
3	Ba	127	867	557.75	390
4	Co	0.5	41	6.03	29
5	Cr	49	97	75	122
6	Cu	4	42	23.69	68
7	Ga	0.6	21	7.44	19
8	Nb	3	96	23	20
9	Ni	5	13	8.44	99
10	Pb	1	18	7.73	13
11	Rb	101	370	237.13	78
12	Sn	8	271	61	2.1
13	Sr	236	511	403.88	384
14	Ta	16	343	146.5	1.7
15	Th	2	19	8.25	8.1
16	U	5	15	8.88	2.3
17	V	7	94	30.56	136
18	Y	1	41	16.78	31
19	Zn	6	35	14.56	76
20	Zr	102	215	124.56	162

*Crustal abundance values after Fortescue, 1992; Parker, 1967.

Spider plot – Primitive mantle (McDonough and Sun 1995)

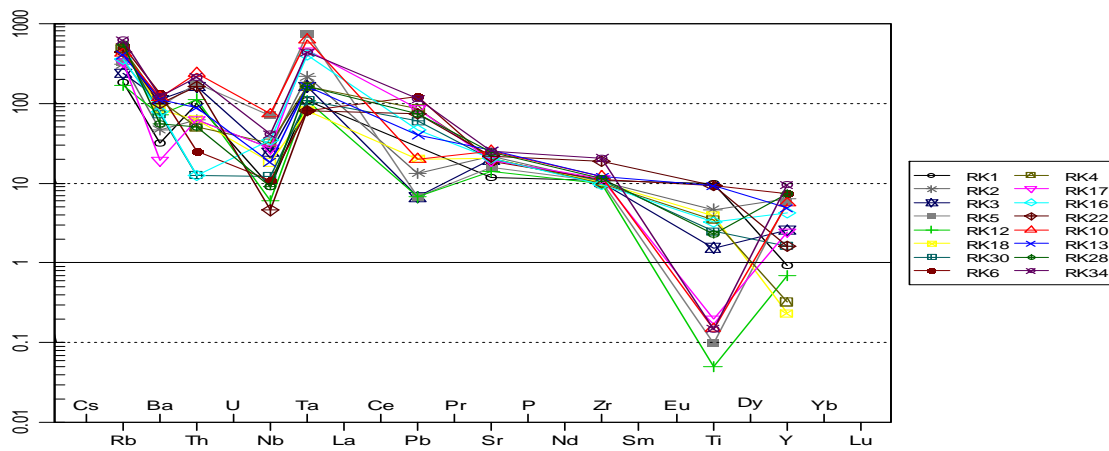


Figure 14. Spider plot-Primitive Mantle (McDonough and Sun 1995)

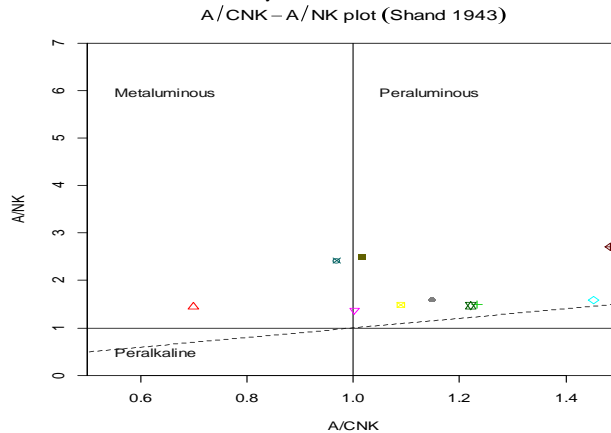


Figure:15 A/NK against ASI plot for granite samples of study area.

Base metals ratio used as fingerprints in understanding the origin, mineralization and evolution of rocks

According to Table 5, trace elements ratio, every sample had Rb/Nb ratio greater than 4.8 ppm. As a result, they are indicating fractionated bed rocks that have a high chance of containing lithium mineralization. Since lithium-bearing pegmatites are enriched in the incompatible elements Li, Cs, Sn, Rb, and Ta, they are frequently referred to as lithium-cesium-tantalum (LCT) pegmatites (Andarawus et al., 2023c). The outcome matches what was discovered during the geochemistry of main oxides and trace elements. The samples indicate that fractionation frequently results in a high Rb/Nb ratio in granites associated with mineralization (Table 4). Rb/Nb levels have been found to increase from a copper deposit's perimeter to its center (Andarawus et al., 2023c). Recently, the ratios of Mg/Fe, Cr/Al, and Ca/Na have been used to make detailed interpretations pertinent to the genesis of mineralizations and metal distributions in chromite, orthopyroxene, and plagioclase in drill cores from Merensky Reef. This has helped to understand the chemical and mineralogical expressions of processes at both large and local scales (Meima et al., 2022). Although crust-derived magmas usually record silica content in excess of 60% (Frost & Shive, 1986), the analyzed rock reported > 60%, which raises some issues about the rock's intermediate compositional concentration of SiO₂. The rock samples were classified using a variety of discrimination TAS diagrams given below based on the concentration of main oxides (Figure 16). The medium grained biotite granite samples map in the field of granite on the TAS diagram following Cox et al. (1979). Granodiorites are primarily found in the quartz diorite (or granodiorites) field on the SiO₂ versus Na₂O+K₂O plot (Figure 16), which was created by Cox et al., (1979).

Degree of fractional crystallization in relation to SiO₂ vs Na₂O, K₂O, CaO, MgO, TiO₂, P₂O₅

The degree of fractional crystallization is determined using the Harker's variation diagram, by plotting Al₂O₃ Vs SiO₂, Na₂O Vs SiO₂, K₂O Vs SiO₂, CaO Vs SiO₂, MgO Vs SiO₂, TiO₂ Vs SiO₂, and FeO_t Vs SiO₂, also, to show the geochemical relationship of the major oxides as the rocks evolves and fractionate. This reveals a substantial alteration and contamination during the magma ascension, as the plots indicates nonlinear trends (Figure 17). Therefore, primary mineralogical assemblages must have seen substantial alterations throughout fractionation, as indicated by the scattered/nonlinear trend in the plots. According to petrogenetic analysis, the granitoids in the study area were formed from a syn-to- within a tectonic environment associated to plate collisions and have a shared genetic origin through fractional crystallization.

Table 5: Element ratio and sum of some oxides in the area

S/N	Sample	Rb/Nb	K ₂ O/NO	Na ₂ O/Al ₂ O ₃	K ₂ O/Al ₂ O ₃	Na ₂ O/K ₂ O	Na ₂ O+K ₂ O	Na ₂ O+K ₂ O O-CaO	Al ₂ O ₃ /CaO+ Na ₂ O+K ₂ O	Al ₂ O ₃ /Na ₂ O O+K ₂ O	Zr/TiO ₂	Y+Nb
1	RK1	9.03	1.68966	0.040559	0.068532	0.591836	1.56	-2.95	2.3558	9.16666	56.218 9	10
2	RK2	10.22	2.09244	0.176558	0.369436	0.477912	7.36	1.87	1.049	1.83153	117.02 18	45
3	RK3	8.88	2.37441	0.159125	0.377828	0.421158	7.12	6.1	1.6289	1.86236	331.25	27
4	RK5	4.37	1.88318	0.146075	0.275085	0.531017	6.17	6.02	2.318	2.37439	5550	71
5	RK12	25.25	2.42584	0.147912	0.358811	0.412229	7.16	6.72	1.8592	1.97346	10.4	7
6	RK18	25.16	0.47664	0.336267	0.160277	2.098039	7.9	5.53	1.5491	2.01392	138.46 15	13
7	RK30	36.63	2.09958	0.171286	0.35963	0.476285	7.47	5.56	1.5	1.88353	226	15
8	RK6	44.43	1.57143	0.032623	0.051265	0.636364	1.26	-3.46	2.5117	11.9206	63.440 86	39
9	RK4	13.67	0.51452	0.167594	0.086231	1.943548	3.65	1.24	2.3729	3.93973	147.14 28	22.4
10	RK17	11	2.55	0.154278	0.393408	0.392157	7.81	6.72	1.6022	1.82586	3025	28.5
11	RK16	9.22	0.10084	0.158035	0.082337	1.919351	2.62	0.27	3.0301	4.16022	156.92 3	41
12	RK22	87	0.70196	0.172181	0.120864	1.424581	4.34	-0.61	1.5788	3.41242	106.48 65	10
13	RK10	5.25	1.80672	0.164478	0.297167	0.553488	6.68	6.54	2.1217	2.16617	4233.3 33	72
14	RK13	20.08	0.69084	0.166985	0.11536	1.447514	4.43	-0.61	1.1648	3.54176	68.108 11	33
15	RK28	5.24	2.14285	0.157933	0.338428	0.466667	6.82	-4.97	1.5848	2.01466	258.69 6	38
16	RK34	6.49	1.8009	0.154007	0.277352	0.555277	6.19	6.07	2.2742	2.31825	7166.6 66	68

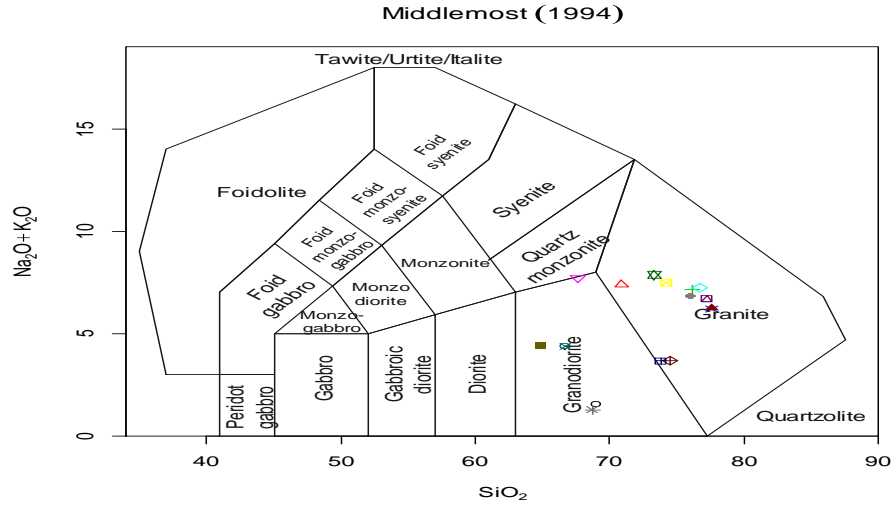


Figure 16: Plot of Middlemost (1994) $\text{Na}_2\text{O} + \text{K}_2\text{O}$ vs SiO_2

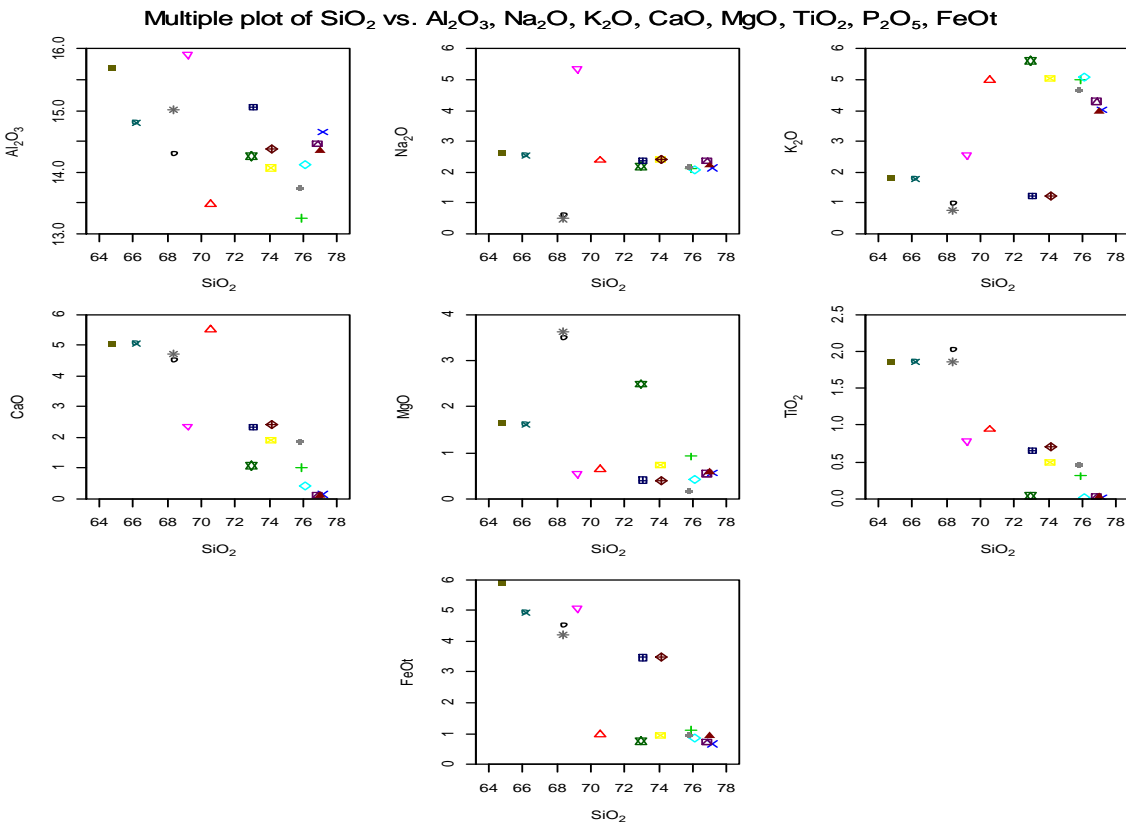


Figure 17: Harker's Multiple Plot of SiO_2 vs Na_2O , K_2O , CaO , MgO , TiO_2 , P_2O_5 ,

CONCLUSION

The study involves the characterization of pegmatites containing tin and tantalum and other rocks from the Chessu area in North Central Nigeria in terms of structure, chemistry, and petrography. Medium-grained banded gneiss, pegmatite, granodiorite, and fine to medium-grained granite gneiss are the rocks observed in the study area. Geologic features such as joint sets, pygmatic and related folds, as well as sinistral and dextral faults, are evidence of the severe deformation events that have occurred in these rocks. Tectonically, the region exhibits NE-SW, and NE-SW, with 40° to 45° dips being the most common. The most prevalent minerals present in the rocks include opaque minerals, muscovite, biotite, quartz, plagioclase, and orthoclase. The main oxides are Al₂O₃, TiO₂, SiO₂, MgO, MnO, Na₂O, P₂O₅, Fe₂O₃, K₂O, and CaO. Tin (Sn), arsenic (As), zircon (Zr), rubidium (Rb), yttrium (Y), niobium (Nb), barium (Ba), tantalum (Ta), and silver (Ag) are among the trace and base metals that have concentrations higher than their background levels. The Rb/Nb ratio in all of the samples is greater than 4.08 ppm, suggesting fractionated bed rocks with a high potential for the occurrence of lithium. Thorium (Th), rubidium (Rb), niobium (Nb), tantalum (Ta), strontium (Sr), and depletion in Ti and Y while Zr and Sr are shown in a spider plot, which show that the environment has an unusually high concentration of enrichment components. This could therefore result in the formation of columbite and tantalite, as well as Sn. The primary mineralogical assemblages of the rocks in the study area must have seen substantial alterations throughout fractionation, as indicated by the non-linear trend they show on Harker plots. According to petrogenetic analysis, the granitoids in the study area were formed from a syn-to-within a tectonic environment associated with plate collisions and have a shared genetic origin through fractional crystallization.

Recommendation

It is recommended that further characterization studies be conducted including the use of X-ray diffraction (XRD), scanning electron microscopy (SEM), electron probe micro-analysis (EPMA) etc. Isotopic investigation and fluid inclusion studies are also recommended to constrain the origin of the ore in the study area. Also, detailed geophysical investigation should be carried out to better determine the magnitude and extent of the pegmatites.

Conflict of interest

The authors declare no conflict of interests.

Acknowledgement

A.S. Usman thank the organizers of the Second International Conference (Abuja 2024) of the Nigerian Association of Exploration Geophysicists for Geoscientist and Engineers (NAEG), where part of this work was presented. Some of the comments and constructive criticism provided during the presentation partly improved this work.

REFERENCES

- Ananaba, S. E & Ajakaiye, D. E (1987). Evidence of tectonic control of mineralization in Nigeria from lineament density analysis A Landsat-study. *International Journal of Remote Sensing*. **8**:1445–1453.
- Andarawus, Y., Likkason, O. K., Sadiq, M. A., Sani, A., Aliyu, M. K., & Anzaku, I. Y.(2023a). Lineaments Characterization and their Tectonic Significance in Mineralization using Landsat TM Data and Field Studies along Mambilla Plateau, Northeast, Nigeria. *Dutse Journal of Pure and Applied Sciences (DUJOPAS)*, Vol. 9 No. 4a, pp12-29.
- Andarawus, Y., Likkason, O. K., Sadiq, M. A., Ali, S., Shekwonyadu, I., Abubakar, A., & Ibrahim, A. A. (2023c). Integrating Remote Sensing Data with Hydrothermal Alteration Mapping and Geochemical Characteristics of Precambrian Rocks across Mambilla Plateau, Northeastern, Nigeria. *FUDMA Journal of Sciences*, 7(5), pp328-347.
- Anudu G.K, Obrike S.E, Iyakwari S. and Ekpokonte A.E. (2010): Preliminary structural study of landsat imagery over Wamba and its environs Nasarawa state North central Nigeria. *Research Journal of Applied Sciences* 7: 1-9.
- Auken E, Pellerin L, Christensen NB & Sørensen K (2006). A survey of current trends in near surface electrical and electromagnetic methods. *Geophys*. 71(5): G249-G260.
- Azmi, H.; Moarefvand, P & Maghsoudi, A (2021). Gold anomaly ranking based on stream sediment geochemistry in the Fariman–Kashmar axis, NE Iran. *Acta Geochim.*, 40, 135–149.
- Balaram V & Sawant.S.S(2022). Indicator Minerals, Pathfinder Elements, and Portable Analytical Instruments in Mineral Exploration Studies, *Minerals*, 12, 394.
- Bassey, N. E. (2006). Tectonic synthesis of structural data from Uba area in Hawal Basement Northeastern Nigeria. *Global Journal of geological sciences*, **4**(2), 193-197.
- Chakraborty, R.; Kereszturi, G.; Durance, P.; Pullanagari, R.; Ashraf, S & Anderson, C (2020). Biogeochemical Exploration of Gold Mineralization and its Pathfinder Elements Using Hyperspectral Remote Sensing. In *Proceedings of the IGARSS 2020—2020*.
- Chapman, R. J., Allan, M. M., Mortensen, J. K., Wrighton, T.M & Grimshaw, M. R., (2017). A new indicator mineral methodology based on a generic Bi-Pb-Te-S mineral inclusion signature in detrital gold from porphyry and low/intermediate sulfidation epithermal environments in Yukon Territory, Canada. *Miner. Deposita*. **53**:815–834.
- Cox, K. G., Bell, J. D and Pankhurst, R. J. (1979). *The Interpretation of Igneous Rocks*. George, Allen and Unwin, London
- Dada, S.S. (2008): Proterozoic Evolution of the Nigeria-Borborema Province,” In: R. J. Pankhurst, R. A. Trouw, B. B. Brito Neves and M. J. De Wit, Eds., *West Gondwana: Pre-Cenozoic Correlations across the South Atlantic Region*, Geological Society of London Special Publication, London, pp. 121-136.
- Fortescue, J. A. C. (1992). Landscape geochemistry: Retrospect and prospect – 1990. *Applied Geochemistry* **7**: 1–53.

- Frost, B. R & Shive P. N. (1986). Magnetic mineralogy of lower magnetic crust. *Journal of Geophysics and Resistance*, **91**: 6513–6521.
- Harker, A. (1990). The natural history of igneous rocks. Methuen, London.
- Lowrie, W & Fichtner A. (2020). Fundamentals of geophysics, Cambridge University Press.
- McClenaghan, M. B (2005). Indicator mineral methods in mineral exploration. *Geochemical Exploration and Environmental Analysis* **5**:233–245.
- Mc Donough and Sun (1995): chemical differentiation of the earth, relationship between mantle, continental crust and oceanic crust, primitive mantle geochemistry.
- Meima, J. A, Rammlmair, D & Junge, M (2022). The use of Laser Induced Breakdown Spectroscopy for the mineral chemistry of chromite, orthopyroxene and plagioclase from Merensky Reef and UG-2 chromitite, Bushveld Complex, South Africa *Chemical and Geology* **589**:120–686
- Middlemost (1994): rock plot for rock classification
- Mohamed. B. S (2022). Geochemical and Petrological Survey in Northern Ethiopia Basement Rocks for Investigation of Gold and Base Metal Mineralization in Finarwa Area and Its Surrounding Southeast Zone of Tigray, Ethiopia, *American Journal of Geospatial Technology (AJGT)*,1(1) 15-28.
- Mu’awiya, B. A., Christopher, S. D., Nanfa, C. A., Dahiru, A. T., Yohanna, A., Musa, N., & Tobias, S. (2022). Petrography and heavy mineral studies of Lokoja formation along Mount Patti North Central Nigeria: implication for provenance studies. *European Journal of Environment and Earth Sciences*, 3(2), 36-51.
- Nanfa, A. C., Aigbadon, G. O., Christopher, S. D., Friday, I. E., Yohanna, A., Ibrahim, A., ... & Tobias, S. (2023). Geology, Geochemical and Petrographic Studies of Lokoja Sandstone Facies: Implications on Source Area Weathering, Provenance and Tectonic Settings. *Communication in Physical Sciences*, 9(4).
- Odinaka, A. C., Dalom, C., Auduson, A. E., Yohanna, A., Balogun, F. O., Musa, N., ... & Ogunsanya, T. I. (2023). Petrographic Studies of Migmatite-Gneiss, Quartzites and Pegmatites Complex in Crusher Area of Lokoja, Kogi State, Nigeria. *Communication in Physical Sciences*, 10(I).
- Ombiro S & Akisa D (2016). The complexity and uncertainty involved in mine planning and design. Annual proceedings of Sustainable Research and Innovation Conference. 250-252
- Parker, C. A (1967). Fluorescence and Phosphorescence Analysis, *Admiralty materials laboratory, holtonhearn, poole, dorset* **4**(5):456
- Paulen, R.C; Paradis, S.; Plouffe, A & Smith, I.R (2009). Base metal exploration using indicator minerals in glacial sediments, northwestern Alberta, Canada. In Proceedings of the 24TH International Applied Geochemistry Symposium, Fredericton, NB, Canada, 1–4; pp. 557–560.
- Singh, L.G. and Vallinayagam, G. (2012). Petrological and Geochemical Constraints in the Origin and Associated Mineralisation of A- Type Granite Suite of the Dhiran Area, Northwestern Peninsular India. *Geosciences*, 2 (4), 66 – 80.

Publication of the European Centre for Research Training and Development -UK

- Ustamer, P.A. (1999). Pre – early Ordovician Cadomian arc – type granitoids, the Bolu Massif, West Pontides, Northern Turkey: Geochemical Evidence. *International Journal of Earth Sciences*, 88, 2 – 12.
- Vallee M.A, Smith R.S & Keating P (2011). Metalliferous mining geophysics–State of the art after a decade in the new millennium. *Geophys.* 76(4): W31-W50.
- White, A.J.R. and Chappell, B.W. (1977). Ultrametamorphism and Granitoid Gneiss. *Tectonophysics*, 4, 7 – 88.